



## 1 **Cost-benefit analysis of coastal flood defence measures in the North** 2 **Adriatic Sea**

3 Mattia Amadio<sup>1</sup>, Arthur H. Essenfelder<sup>1</sup>, Stefano Bagli<sup>2</sup>, Sepehr Marzi<sup>1</sup>, Paolo Mazzoli<sup>2</sup>, Jaroslav Mysiak<sup>1</sup>,  
4 Stephen Roberts<sup>3</sup>

5 <sup>1</sup> *Centro Euro-Mediterraneo sui Cambiamenti Climatici, Università Ca' Foscari Venezia, Italy*

6 <sup>2</sup> *Gecosistema, Rimini, Italy*

7 <sup>3</sup> *The Australian National University, Canberra, Australia*

### 8 **Abstract**

9 The combined effect of global sea level rise and local subsidence phenomena poses a major threat to coastal  
10 settlements. Flooding events are expected to grow in frequency and magnitude, increasing the potential  
11 economic losses and costs of adaptation. In Italy, a large share of the population and economic activities are  
12 located along the coast of the peninsula, although risk of inundation is not uniformly distributed. The low-  
13 lying coastal plain of Northeast Italy is the most sensitive to relative sea level changes. Over the last half a  
14 century, the entire north-eastern Italian coast has experienced a significant rise in relative sea level, the main  
15 component of which was land subsidence. In the forthcoming decades, sea level rise is expected to become the  
16 first driver of coastal inundation hazard. We propose an assessment of flood hazard and risk linked with  
17 extreme sea level scenarios, both under historical conditions and sea level rise projections at 2050 and 2100.  
18 We run a hydrodynamic inundation model on two pilot sites located in the North Adriatic Sea along the  
19 Emilia-Romagna coast: Rimini and Cesenatico. Here, we compare alternative risk scenarios accounting for the  
20 effect of planned and hypothetical seaside renovation projects against the historical baseline. We apply a flood  
21 damage model developed for Italy to estimate the potential economic damage linked to flood scenarios and  
22 we calculate the change in expected annual damage according to changes in the relative sea level. Finally,  
23 damage reduction benefits are evaluated by means of cost-benefit analysis. Results suggest an overall  
24 profitability of the investigated projects over time, with increasing benefits due to increased probability of  
25 intense flooding in the next future.

26 **Key-words:** coastal inundation Italy extreme sea level rise

27 **Abbreviations:** MSL (Mean Sea Level); TWL (Total Water Level); ESL (Extreme Sea Level); SLR (Sea Level  
28 Rise); VLM (Vertical Land Movements); DTM (Digital Terrain Model); EAD (Expected Annual Damage)

### 29 **1. Introduction**

30 Globally, more than 700 million people live in low-lying coastal areas (McGranahan et al. 2007), and about  
31 13% of them are exposed to a 100-year return period flood event (Muis et al. 2016). On average, one million  
32 people located in coastal areas are flooded every year (Hinkel et al. 2014). Coastal flood risk shows an  
33 increasing trend in many places due to socio-economic growth (Bouwer 2011; Jongman et al. 2012b) and land  
34 subsidence (Syvitski et al. 2009; Nicholls and Cazenave 2010), but in the near future sea level rise (SLR) will  
35 likely be the most important driver of increased coastal inundation risk (Hallegatte et al. 2013; Hinkel et al.  
36 2014). Evidences show that global sea level has risen at faster rates in the past two centuries compared to the  
37 millennial trend (Kemp et al. 2011; Church and White 2011), topping 3.2 mm per year in the last decades  
38 mainly due to ocean thermal expansion and glacier melting processes (Mitchum et al. 2010; Meyssignac and  
39 Cazenave 2012). According to the IPCC projections, it is very likely that, by the end of the 21st century, the  
40 SLR rate will exceed that observed in the period 1971-2010 for all Representative Concentration Pathway (RCP)  
41 scenarios (IPCC 2019); yet the local sea level can have a strong regional variability, with some places



42 experiencing significant deviations from the global mean change (Stocker et al. 2013). This is particularly  
43 worrisome in regions where changes in the mean sea level (MSL) are more pronounced, considering that even  
44 small increases of MSL can drastically change the frequency of extreme sea level (ESL) events, leading up to  
45 situations where a 100-year event may occur several times per year by 2100 (Carbognin et al. 2009, 2010;  
46 Vousdoukas et al. 2017, 2018; Kirezci et al. 2020). Changes in the frequency of extreme events are likely to  
47 make existing coastal protection inadequate in many places, causing a large part of the European coasts to be  
48 exposed to flood hazard. Under these premises, coastal floods threaten to trigger devastating impacts on  
49 human settlements and activities (Lowe et al. 2001; McInnes et al. 2003; Vousdoukas et al. 2017). In this context,  
50 successful coastal risk mitigation and adaptation actions require accurate and detailed information about the  
51 characterisation of coastal flood hazard and the performance of alternative coastal defence options. Cost-  
52 benefit analysis (CBA) is widely used to evaluate the economic desirability of a DRR project (Jonkman et al.  
53 2004; Mechler 2016; Price 2018). CBA helps decision-makers in evaluating the efficacy of different adaptation  
54 options (Kind 2014; Bos and Zwaneveld 2017).

55 In this study, designed coastal renovation projects in the municipalities of Rimini and Cesenatico, in Italy, are  
56 compared against the baseline scenario in terms of net benefits under changing climate conditions. First, we  
57 employ the 2D-hydrodynamic ANUGA model (Roberts et al. 2015) for simulating coastal inundation scenarios  
58 associated with ESL projections over the two pilot areas located along the Emilia-Romagna coast (North  
59 Adriatic Sea). Flood hazard maps are produced for current conditions (2020) and future conditions (2050 and  
60 2100) by combining the local data from historical ESL events with the estimates of relative mean sea level  
61 (RMSL) change for those locations. RMSL change accounts for both the eustatic global rise and the locally-  
62 measured land vertical movement effect. Each inundation scenario simulated by the model is translated in  
63 terms of direct economic impacts using a locally-calibrated damage model. The combination of different risk  
64 scenarios in a CBA framework allows to estimate the economic benefits brought by the project implementation  
65 in terms of avoided direct flood losses up to the end of the century.

## 66 2. Area of study

67 Located in the central Mediterranean Sea, the Italian peninsula has more than 7,500 km of coasts, hosting  
68 around 18% of the country population (ISTAT), numerous towns and cities, industrial plants, commercial  
69 harbours and touristic activities, as well as cultural and natural heritage sites. Existing country-scale estimates  
70 of SLR up to the end of this century helps to identify the most critically exposed coastal areas of Italy (Lambeck  
71 et al. 2011; Bonaduce et al. 2016; Antonioli et al. 2017; Marsico et al. 2017). The North Adriatic coastal plain is  
72 acknowledged to be the largest and most vulnerable location to extreme coastal events due to the shape,  
73 morphology and low bathymetry of the Adriatic sea basin, which cause water level to increase relatively fast  
74 during coastal storms (Carbognin et al. 2010; Ciavola and Coco 2017; Perini et al. 2017). The ESL here is driven  
75 mainly by astronomical tide, ranging about one meter in the *northernmost* sector, and meteorological forcing,  
76 such as low pressure, seiches and prolonged rotational wind systems, which are the main trigger of storm  
77 surge in the Adriatic basin (Carbognin et al. 2010; Vousdoukas et al. 2017). In addition to that, all the coastal  
78 profile of the Padan plain shows relatively fast subsiding rates, partially due to natural phenomena, but in  
79 large part linked to human activities. We focus our analysis on two pilot sites located along the Adriatic coast  
80 of Emilia-Romagna, shown in figure 1: Cesenatico and Rimini.



81  
82 **Figure 1.** Pilot areas locations along the Emilia-Romagna coast: Cesenatico and Rimini. The coastal defence  
83 structure assessed in this study are shown in black. Buildings footprint data from Regional Environmental  
84 Agency (ARPA) 2020. Basemap © Google Maps 2020.

85 The number of annual ESL events reported along the Emilia-Romagna coast shows a steady increase since the  
86 second half of the past century (Perini et al. 2011), which is in part explained by to the socio-economic  
87 development of the coast. The landscape along the 130 km regional coastline is almost flat, the only relief being  
88 old beach ridges, artificial embankments and a small number of dunes. The coastal perimeter is delineated by  
89 a wide sandy beach that is generally protected by offshore breakwaters, groins and jetties. The land elevation  
90 is often close to (or even below) the MSL, while the coastal corridor is heavily urbanised. Cesenatico has about  
91 26,000 residents, while Rimini has 150,000. These port towns have a strong touristic vocation, hosting large  
92 beach resort and bathing facilities along the beach and hundreds of hotels and rental housing located just  
93 behind the seaside. Both towns are affected by beach erosion and the regression of the coastline, and on several  
94 occasions they suffered from coastal storms resulting in flooding of buildings and activities. In some cases, the  
95 storm surge obstructed the river outlets causing the overflow of channels and the flooding of surrounding  
96 areas (Perini et al. 2011).

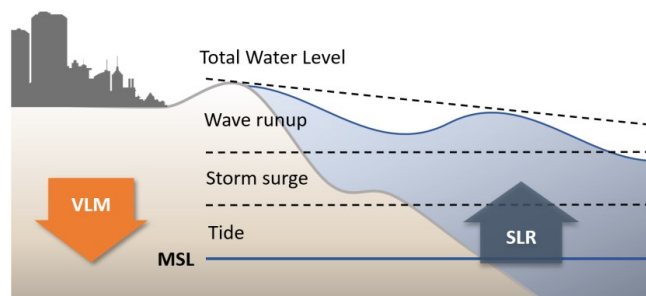
### 97 3. Methodology

#### 98 3.1 Components of the analysis

99 Coastal inundation phenomena are caused by an increase of total water level (TWL), most often associated to  
100 extreme sea level (ESL) events, which are generated by a combination of high astronomical tide and  
101 meteorological drivers such as storm surge and wind waves (figure 2). Estimates of ESL are obtained for the  
102 North Adriatic up to year 2100 by combining reference hazard scenarios derived from historical records with  
103 regionalised projections of SLR (Vousdoukas et al. 2017) and local vertical land movements (VLM) rates. Four  
104 ESL frequency scenarios, namely once in 1, 10, 100- and 250-years, are considered. The hydrodynamic model  
105 ANUGA is applied to simulate the inundation of land areas during ESL accounting for individual components



106 (storm surge, tides and waves). Land morphology and exposure of coastal settlements are described by high-  
107 resolution DTM and bathymetry, in combination with land use and buildings footprints. The effect of hazard  
108 mitigation structures (both designed and under construction) are explicitly accounted in the “defended”  
109 simulation scenario, in contrast to the baseline scenario, where only existing defence structures (groins, jetties,  
110 breakwaters and sand dunes) are accounted.



111

112 **Figure 2.** Components of the analysis for extreme sea level events: total water level is calculated as the sum of  
113 tide, storm surge and wave runup over mean sea level. Vertical land movement and eustatic sea level rise  
114 affects the mean sea level on the long run.

### 115 3.2 Vertical Land Movement

116 Vertical land movements result from a combination of slow geological processes such as tectonic activity and  
117 glacial isostatic adjustment (Peltier 2004; Peltier et al. 2015), and medium-term phenomena, such as sediment  
118 loading and soil compaction (Carminati and Martinelli 2002; Lambeck and Purcell 2005). The latter can greatly  
119 oversize geological processes at local scale (Wöppelmann and Marcos 2012); in particular, faster subsidence  
120 occurs in presence of intense anthropogenic activities such as water withdrawal and natural gas extraction  
121 (Teatini et al. 2006; Polcari et al. 2018). Most of the peninsula shows a slow subsiding trend, although with  
122 some local variability. An estimate of VLM rates due to tectonic activity have been derived from studies  
123 conducted in Italy (Lambeck et al. 2011; Antonioli et al. 2017; Marsico et al. 2017; Solari et al. 2018). The North  
124 Adriatic coastal plain shows the most intense long-term geological subsidence rates (about 1 mm per year),  
125 increasing North to South. Yet in the last decades these rates were often greatly exceeded by ground  
126 compaction rates observed by multi-temporal SAR Interferometry (Gambolati et al. 1998; Antonioli et al. 2017;  
127 Polcari et al. 2018; Solari et al. 2018). Observed subsidence is about one order of magnitude faster where the  
128 aquifer system has been extensively exploited for agricultural, industrial and civil use since the post-war  
129 industrial boom. From the 1970s, however, with the halt of groundwater withdrawals, anthropogenic  
130 subsidence has been strongly reduced or stopped, but many of the induced effects still remain (Carbognin et  
131 al. 2009). Geodetic surveys carried out from 1953 to 2003 along the Ravenna coast provide evidence of a  
132 cumulative land subsidence exceeding 1 m at some sites due to gas extraction activities. Average subsidence  
133 rates observed for 2006-2011 along the Emilia-Romagna coast are around 5 mm/yr, exceeding 10 mm/yr in the  
134 back shore of the Cesenatico and Rimini areas and topping 20-50 mm/yr in Ravenna (Carbognin et al. 2009;  
135 Perini et al. 2017). Based on these current rates, we assume an average fixed annual VLM of 5 mm in both  
136 Cesenatico and Rimini up to the end of the century. This remarkable difference between natural VLM rates  
137 and observations would produce a dramatic effect on the estimated SLR scenarios: at present rates, Rimini  
138 would see an increase of MSL by 0.15 m in 2050 and more than 0.4 m in 2100 independently from eustatic SLR.  
139 Since these rates are connected with human activity, it is not possible to foresee exactly how they will change  
140 in the long term.



### 141 3.3 Sea Level Rise

142 The long availability of tide gauge data along the N Adriatic coast allows to assess the changes in MSL in the  
143 last century. Records from the gauge station of Marina di Ravenna show an eustatic rise of 1.2 mm per year  
144 from 1890 to 2007, in good agreement with the eustatic rise measured at other stations in the Mediterranean  
145 Sea (Tsimplis and Rixen 2002; Carbognin et al. 2009). The projections of future MSL account for sea thermal  
146 expansions from four global circulation models, estimated contributions from ice-sheets and glaciers (Hinkel  
147 et al. 2014) and long-term subsidence projections (Peltier 2004). The ensemble mean is chosen to represent each  
148 RCP for different time slices. The increase in the central Mediterranean basin is projected to be approximately  
149 0.2 m by 2050 and between 0.5 and 0.7 m by 2100, compared to historical mean (1970-2004) (Vousdoukas et al.  
150 2017). We consider the intermediate emission scenario RCP 4.5 (Thomson et al. 2011), projecting an increase  
151 in MSL of 0.53 m at 2100. It must be noted that these projections, although downscaled, do not account for the  
152 peculiar continental characteristics of the shallow northern Adriatic sector, where the hydrodynamics and  
153 oceanographic parameters partially depend on the freshwater inflow (Zanchettin et al. 2007).

### 154 3.4 Tides and meteorological forcing

155 Storm surge and strong waves represents the largest contribution to TWL during an ESL event. An estimation  
156 of these components is obtained for the pilot sites from the analysis of tide gauge and buoy records, and from  
157 the description of historical extreme events presented in local studies (Perini et al. 2011, 2012, 2017; Masina et  
158 al. 2015; Armaroli and Duo 2018). This area is microtidal: the mean neap tidal range is 30–40 cm, and the mean  
159 spring tidal range is 80–90 cm. Most storms have a duration of less than 24 h and a maximum significant wave  
160 height of about 2.5 m. During extreme cyclonic events, the sequence of SE wind (*Sirocco*) piling the water North  
161 and E-NE wind (*Bora*) pushing waves towards the coast can generate severe inundation events, with  
162 significant wave height ranging 3.3 – 4.7 m and exceptionally exceeding 5.5 m (Armaroli et al. 2012). Fifty  
163 significant events have been recorded from 1946 to 2010 on the ER coast, with half of them causing severe  
164 impacts along the whole coast and 10 of them being associated with important flooding events (Perini et al.  
165 2017). The most severe events are found when strong winds blow during exceptional tide peaks, most often  
166 happening in late autumn and winter. The event of November 1966 represents the highest ESL on records,  
167 causing significant impacts along the regional coast: the recorded water level was 1.20 m above MSL, and  
168 wave heights offshore were estimated around 6–7 m (Perini et al. 2011; Garnier et al. 2018). The whole coastline  
169 suffered from erosion and inundation, especially in the province of Rimini. Atmospheric forcing shown  
170 significant variability for the period 1960 onwards (Tsimplis et al. 2012), but there is no strong evidence  
171 supporting a significant change in trend for the next future (Lionello 2012). Thus, we assume the frequency  
172 and intensity of meteorological events to remain the same up to 2100.

### 173 3.5 Terrain morphology and coastal defence structures

174 Reliable bathymetries and topography are required in order to run the hydrodynamic modelling at the local  
175 scale. Bathymetric data for the Mediterranean area were obtained from the European Marine Observation and  
176 Data Network (EMODnet) at 100 m resolution. The description of terrain morphology comes from the official  
177 high-resolution LIDAR DTM (MATTM, 2019). First, we combined the coastal dataset (2 m resolution and  
178 vertical accuracy of  $\pm 0.2$  m), and the inland dataset (1 m resolution and vertical accuracy  $\pm 0.1$  m) into one  
179 seamless layer. Then, the DTM is supplemented with geometries of existing coastal protection elements such  
180 as jetties, groins and breakwaters obtained from the digital Regional Technical Map. In Rimini, the Parco del  
181 Mare is an urban renovation project which aims to improve the seafront promenade: the existing road and  
182 parking lots are converted into an urban green infrastructure consisting of a concrete barrier covered by  
183 vegetated sandy dunes with walking path. This project also act as a coastal defence system during extreme sea



184 level events. The barrier rises 2.8 meters along the southern section of the town, south of the marina; no barrier  
185 is planned on the northern coastal perimeter. The Parco del Mare project, currently under construction, has  
186 been taken in account in the evaluation of the “defended” scenarios by merging the barrier into the existing  
187 DTM (figure 3).

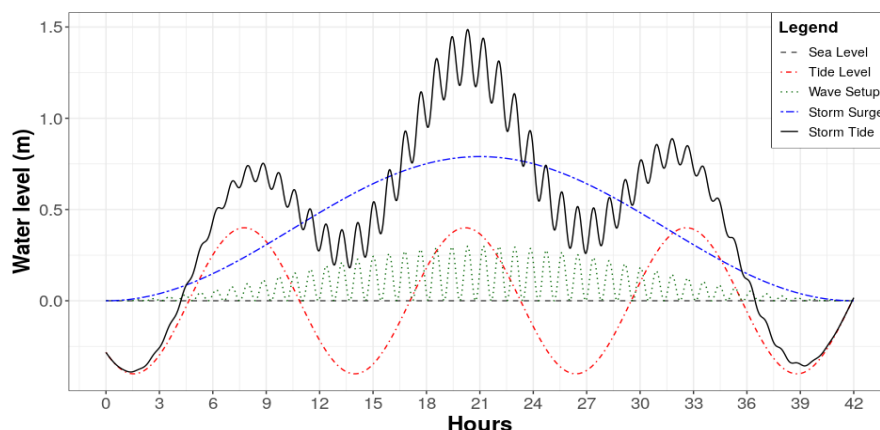


188  
189 **Figure 3.** prototype design of Parco del Mare project in Rimini. Adapted from JDS Architects.

190 In Cesenatico, the existing defence structure include a moving barriers system (*Porte Vinciane*) located on the  
191 port channel, coupled with a dewatering pump which discharge the meteoric waters in the sea. The barriers  
192 close automatically if the TWL surpasses 1 meter over the mean, preventing floods in the historical centre up  
193 to ESL of 2.2 meters. Additional defence structures include the winter dunes, which consist of a 2.2 meter-tall  
194 intermittent, non-reinforced sand barrier. In the defended scenario, we envisage a coastal defence structure  
195 similar to Parco del Mare in Rimini, spanning both north and south of the port channel with a total length of  
196 7.8 km. A proper setup of inundation model required to first perform some manual editing of the DTM using  
197 additional reference data (i.e. on-site observations or aerial photography) in order to produce an elevation  
198 model that realistically represent the land morphology and associated water dynamics (e.g. removal of non-  
199 existent sink holes). Bridges and tunnels are the most critical elements corrected in order to avoid  
200 misrepresentations of the water flow routing.

### 201 3.6 Inundation modelling

202 At the local scale, hydrodynamic models represent an efficient compromise between hydrostatic and hydraulic  
203 models, being able to perform realistic simulations of inundation phenomena and to obtain detailed  
204 information about the hazard features, while requiring a relatively fast setup and reasonable computational  
205 effort. In this study we use ANUGA, a 2D hydrodynamic model originally developed to simulate tsunami  
206 events, which is also suitable for the simulation of hydrologic phenomena such as riverine peak flows and  
207 storm surges (Roberts 2020). The fluid dynamics in ANUGA is based on a finite-volume method for solving  
208 the shallow water wave equations, thus being based on continuity and simplified momentum equation. The  
209 model computes the total water level, the water depth, and the horizontal momentum on an irregular  
210 triangular grid based on the provided forcing conditions. ANUGA includes also an operator module that  
211 simulates the removal of sand associated with over-topping of a sand dune by sea waves, which is applied to  
212 explore scenarios where a sand dune barrier provides protection for the land behind. The operator simulates  
213 the erosion, collapse, fluidisation and removal of sand from the dune system (Kain et al. 2020); the dune  
214 erosion mechanism relies on a relationship based on Froehlich (2002). This option is enabled only in the  
215 undefended scenario for Cesenatico, where non-reinforced sand dunes are prone to erosion.



216  
 217 **Figure 4.** Total Water Level (black) as a sum of tide (red), storm surge (green) and waves (blue) for ESL scenario  
 218 1 in 10 years.

219 TWL on the coastland is modelled at every timestep as the sum of extreme values for storm surge level (*SS*),  
 220 wave runup (*Wr*), and max tide (*Tmax*), as shown in figure 4. The maximum tidal excursion is 0.8 m, while  
 221 wave height can range from 3 to almost 6 m during strong wind events, translated into a wave setup on the  
 222 shore ranging from 0.22 to 0.65 m. Additional details are wave period (*Wp*, in seconds) and event duration  
 223 (Time, in hours), required to estimate the maximum extent of inland water propagation. Wave direction is  
 224 oriented perpendicular to the coast. Storm surge is set to peak in the mid of the event, producing the maximum  
 225 TWL value for the event. The most exceptional ESL events can last up to 3 days. Table 4 summarizes the ESL  
 226 components according to the four probability scenarios identified from local historical records (Perini et al.  
 227 2017). The probability of occurrence is expressed in terms of return period (*RP*), which is the estimated average  
 228 time interval between events of similar intensity. Wave run up is calculated from significant wave height. The  
 229 output of the simulation consists of maps representing flood extent, water depth and momentum at every time  
 230 step (1 second), projected on the high-resolution DTM grid.

231 **Table 1.** components of TWL during an ESL event under historical conditions and projected conditions (2050  
 232 and 2100), accounting for both eustatic SLR (RCP4.5) and average VLM rate.

RP (years)	Extreme event features				Historical	2050			2100		
	SS (m)	Tmax (m)	Wr (m)	Time (h)	TWL (m)	SLR (m)	VLM (m)	TWL (m)	SLR (m)	VLM (m)	TWL (m)
1	0.60	0.40	0.22	32	1.2	0.14	0.19	1.55	0.53	0.44	2.2
10	0.79	0.40	0.30	42	1.5	0.14	0.19	1.82	0.53	0.44	2.5
100	1.02	0.40	0.39	55	1.8	0.14	0.19	2.14	0.53	0.44	2.8
250	1.40	0.45	0.65	75	2.5	0.14	0.19	2.83	0.53	0.44	3.5

233 **3.7 Risk modelling and Expected Annual Damage**

234 Direct damage to physical asset is estimated using a customary flood risk assessment approach originally  
 235 developed for fluvial inundation, which is adapted to coastal flooding assuming that the dynamic of impact  
 236 from long-setting floods depends on the same factors, namely: 1) hazard magnitude, and 2) size and value of  
 237 exposed asset. Indirect economic losses due to secondary effects of damage (e.g. business interruption) are  
 238 excluded from our computation. Hazard magnitude can be defined by a range of variables, but the most  
 239 important predictors of damage are water depth and the extension of the flood event (Jongman et al. 2012a;  
 240 Huizinga et al. 2017). Land cover definitions and buildings footprints help to estimate the exposed capital



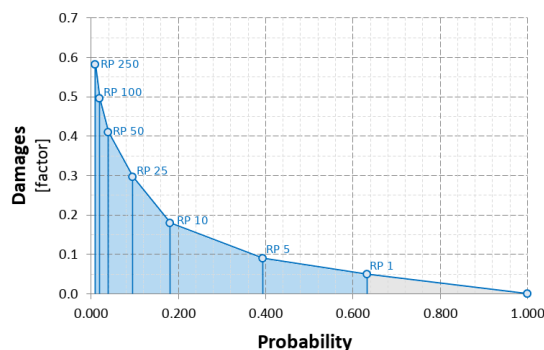
241 including residential buildings, commercial and industrial activities, infrastructures, historical and natural  
 242 sites. The characterization of exposed asset is built from a variety of sources, starting from land use and  
 243 buildings footprints obtained from the Regional Environmental Agencies geodatabases and the Open Street  
 244 Map database (Geofabrik GmbH 2018). Additional indicators about buildings characteristics are obtained  
 245 from the database of the official Italian Census of 2011 (ISTAT), while mean construction and restoration costs  
 246 per building types are obtained from cadastral estimates (CRESME 2014). A depth-damage function  
 247 previously validated on empirical records (Amadio et al. 2019) and then applied in order to translate each  
 248 hazard scenario into an estimate of economic risk, measured as a share of total exposed value. The curve covers  
 249 only residential and mixed-residential buildings; other types (e.g. harbour, industrial, commercial, historical  
 250 monuments and churches) are excluded from risk computation. Abandoned or under-construction buildings  
 251 are excluded from the analysis. To avoid overcounting of marginally-affected buildings, we set two threshold  
 252 conditions for damage calculation: flood extent must be greater than or equal to 10 m<sup>2</sup>, and maximum water  
 253 depth greater than or equal to 10 cm. The damage/probability scenarios are combined together as Expected  
 254 Annual Damage (EAD). EAD is the damage that would occur in any given year if damages from all flood  
 255 probabilities were spread out evenly over time; mathematically, EAD is the integration of the flood risk density  
 256 curve over all probabilities (Olsen et al. 2015), as in equation 1.

$$EAD = \int_0^1 D(p) dp \quad (1)$$

257 The integration of the curve can be solved either analytically or numerically, depending on the complexity of  
 258 the damage function  $D(p)$ . Several different methods for numerical integration exist; we use an approach  
 259 where EAD is the sum of the product of the fractions of exceedance probabilities by their corresponding  
 260 damages. We calculate  $D(p)$ , which is the damage that occurs at the event with probability  $p$ , by using a depth-  
 261 damage function previously validated for Italy on empirical records (Amadio et al. 2019) for each hazard  
 262 scenario. The exceedance probability of each event ( $p$ ) is calculated based on exponential function as shown in  
 263 equation 2.

$$p = 1 - e^{\left(\frac{-1}{RP}\right)} \quad (2)$$

264 Events with a high probability of occurrence and low intensity (below RP 1 year) are not simulated, and  
 265 assumed to not cause significant damage. This is consistent with the historical observations for the case study  
 266 area, although this assumption could change with increasing MSL.



267  
 268 **Figure 5.** Schematic representation of the numerical integration of the damage function  $D(p)$  with respect to  
 269 the exponential probability of the hazard events. Events with a probability of occurrence higher than once in  
 270 a year are expected to not cause damage (grey area).



### 271 3.8 Cost-Benefit Analysis

272 A CBA should include a complete assessment of the impacts brought by the implementation of the hazard  
273 mitigation option, i.e. direct and indirect, tangible and intangible impacts (Bos and Zwaneveld 2017). The  
274 project we are considering, however, has not been primarily designed for DRR purpose: instead, it is meant  
275 as an urban renovation project which aims to improve the fruition of the seafront and the urban landscape.  
276 This implies some large indirect effects on the whole area, most of which are not strictly related to risk  
277 management and, overall, very difficult to estimate ex-ante. Our evaluation focuses only on the benefits  
278 achieved in terms of reduction in direct flood losses. The implementation costs include the initial investment  
279 required for setting up the adaptation measure, and operational costs through time. The initial investment is  
280 estimated to be 6 M Eur per Km. No information is available about operational costs, but given the nature of  
281 the project (static defense with very low fragility to floods), we assume they will be rather small compared to  
282 the initial investment. We account for ordinary annual maintenance costs as 0.1% of the total cost of the opera.  
283 Costs and benefit occurring in the future periods need to be discounted, as people put higher value on the  
284 present (Rose et al., 2007). This is done by adjusting future costs and benefits using an annual discount rate  
285 ( $r$ ). We chose a variable rate of  $r = 3.5$  for the first 50 years and  $r = 3$  from 2050 onward (Lowe 2008). The three  
286 main decision criteria used in CBA for project evaluation are the Net Present Value (NPV), the Benefit/Cost  
287 Ratio (BCR) and the payback period. The NPV is the sum of Expected Annual Benefits ( $B$ ) up to the end of the  
288 time horizon, discounted, minus the total costs for the implementation of the defense measure, which takes  
289 into account initial investment plus discounted annual maintenance costs ( $C$ ). In other words, the NPV of a  
290 project equals the present value of the net benefits ( $NB_i = B_i - C_i$ ) over a period of time (Boardman et al. 2018),  
291 as in equation (3):

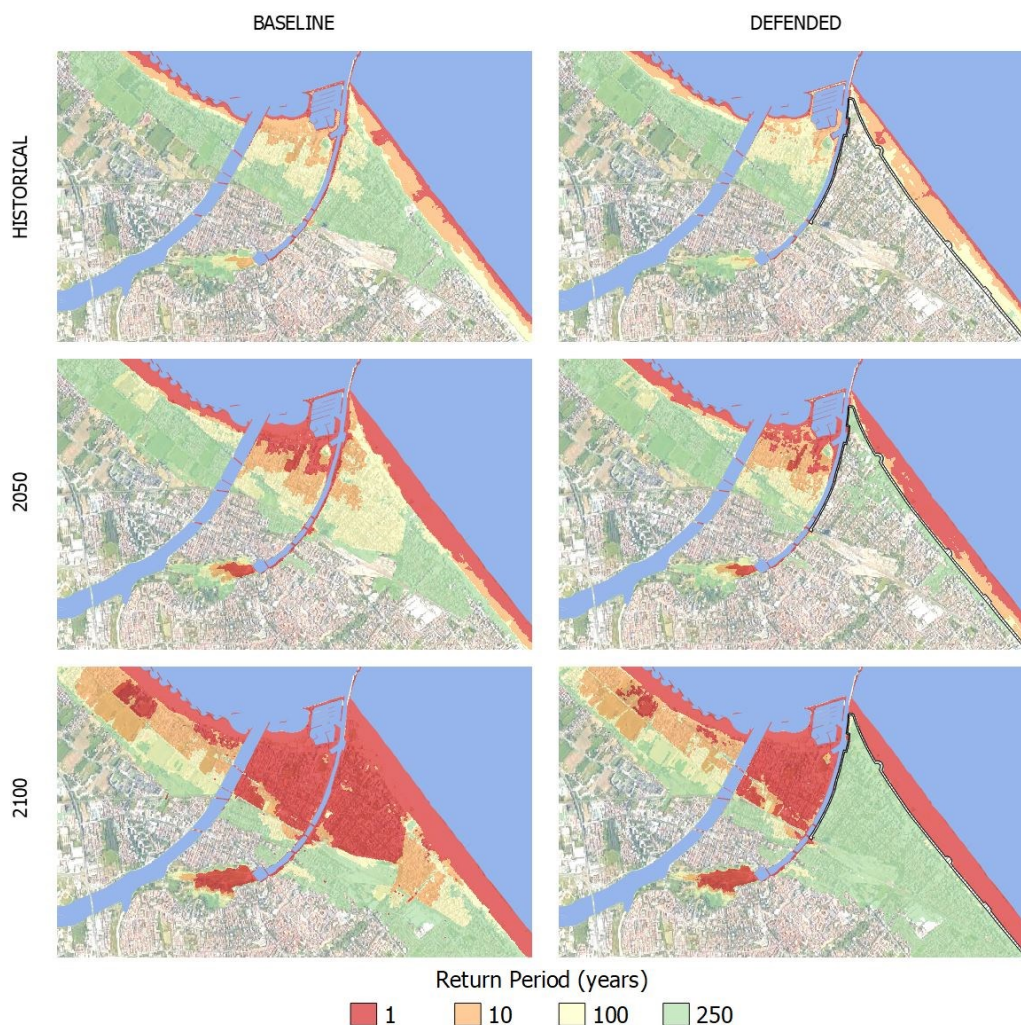
$$NPV = PV(B) - PV(C) = \sum_{t=0}^n \frac{NB_t}{(1+r)^t} \quad (3)$$

292 Positive NPV means that the project is economically profitable. The BCR is instead the ratio between the  
293 benefits and the costs; a BCR larger than 1 means that the benefits of the project exceed the costs on the long  
294 term and the project is considered profitable. The payback period is the number of years required for the  
295 discounted benefits to equal the total costs.

## 296 4. Results

### 297 4.1 Inundation scenarios

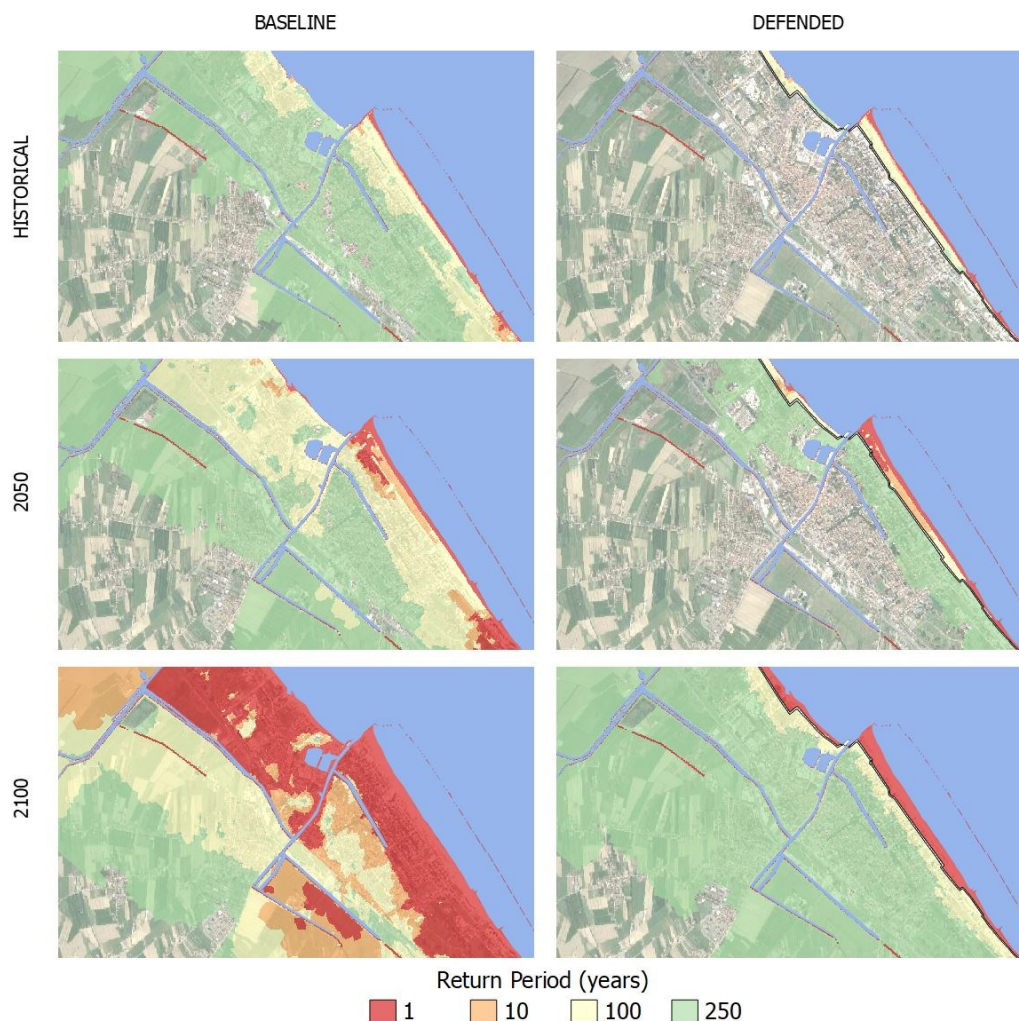
298 Once the setup is completed, the hydrodynamic model performs relatively fast: each simulation is carried at  
299 half speed compared to reality; that means, it takes about 24 hours to simulate a 12 h event. Parallel simulations  
300 for the same area can run on a multicore processor, improving the efficiency of the process. The output of the  
301 hydrodynamic model consists of a set of inundation simulations that include several hazard intensity variables  
302 in relation to flood extent: water depth, flow velocity, and duration of submersion. ESL scenarios are then  
303 summarized into static maps, each one representing the maximum value reached by hazard intensity variables  
304 at grid cell level (about 1 meter) during the whole simulated event. The flood extents corresponding to each  
305 RP scenario are shown for Rimini (figure 5) and Cesenatico (figure 6).



306

307 **Figure 6.** Rimini, extent of land affected by flood according to frequency of occurrence of ESL event up to 2100  
308 for the baseline [left] and the defended scenario [right]. Basemap © Google Maps 2020.

309 In Rimini, the Parco del Mare barrier produces benefits in terms of avoided damage in the south-eastern part  
310 of the town (high-density area) for ESL events with a probability up to 1 in 100 years. The north-western part  
311 and the marina are not affected by the coastal renovation project. In all the simulations, the buildings located  
312 behind the marina are the firsts to be flooded. In fact, the new and the old port channels located on both sides  
313 of the marina represent a hazard hotspot: as shown in the maps, the failure of the eastern channel, which has  
314 a relatively low elevation, is likely to cause the water to flood the eastern part of the town, even during  
315 inundation events that would not surpass the beach perimeter. In the defended scenarios, where both the  
316 coastal and the canal barriers are enabled, the flood extent in the SE urban area becomes almost zero for ESL  
317 events with a probability of once in 100 years, even when accounting for SLR up to 2100. Under more  
318 exceptional ESL conditions (RP 250 in 2100), the barrier is surmounted, generating a flood extent similar to the  
319 baseline scenario.



320

321 **Figure 7.** Cesenatico, extent of land affected by flood according to frequency of occurrence of ESL event up to  
 322 2100 for the baseline [left] and the defended scenario [right]. Basemap © Google Maps 2020.

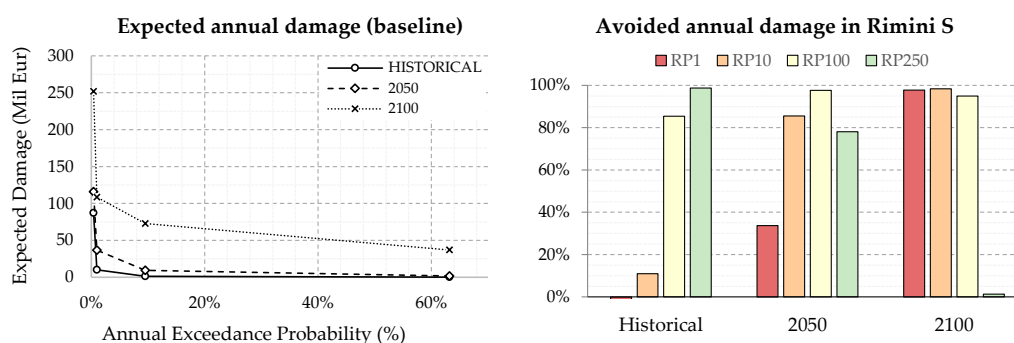
323 In Cesenatico, a barrier designed similarly to Parco del Mare could provide significant reduction of flood  
 324 extents under most hazard scenarios. Its effectiveness would be greater than in Rimini thanks to the  
 325 complementary movable barrier system in use, which seals the port channel allowing to wall off the whole  
 326 coastal perimeter, reducing the chance of water ingression in the urban area. In contrast, the erodible winter  
 327 dune in the baseline defense scenario can only hold the heavy sea for shorter, less intense ESL events, and  
 328 becomes ineffective with more exceptional, long-lasting events; at 2050 and 2100, the winter dune gets  
 329 surmounted and dismantled by sea waves for scenario RP250 years (mid- and low-left maps).

#### 330 4.2 Expected Annual Damage

331 The estimate of expected economic impacts calculated as a function of maximum exposed value, and water  
 332 depth is summarized as Expected Annual Damage in figure 7, left chart. In Rimini, the EAD grows from  
 333 around 650 thousand Eur under historical conditions to 2.8 million Eur in 2050 and more than 32.3 million Eur

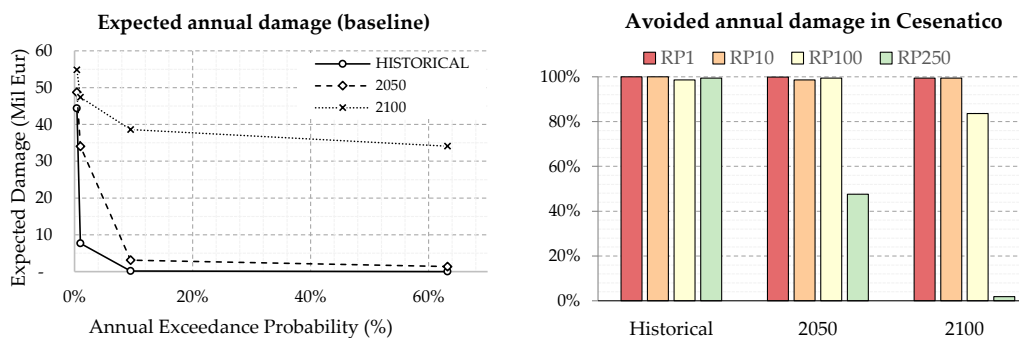


334 in 2100. With less severe events (up to RP 100 years), the risk remains mostly confined around the marina area  
 335 (outside the protection offered by the reinforced dune) producing an EAD below 10 thousand Eur; with higher  
 336 water levels (i.e. RP 250 years), the benefits of the dune barrier protecting the southern part of the town become  
 337 more evident, avoiding about 65% of the EAD. The damage avoided by the barrier in the southern sector  
 338 (Rimini S) grows almost linearly with the increase of EAD under future projections of sea level rise: under the  
 339 defended hypothesis, the EAD is reduced on average by 45%. The project produces benefit up to ESL RP250  
 340 years in 2100, where a projected TWL of 3.5 meters would cause the surmounting of the barrier, reducing the  
 341 benefits to almost zero (figure 7, right).



342  
 343 **Figure 8.** Rimini: Expected Annual Damage (EAD) according to undefended scenario up to 2100 [left]; EAD  
 344 reduction in the South part of the town thanks to hazard mitigation offered by the coastal barrier [right].

345 In Cesenatico, the average EAD for the undefended scenario grows from around 270 thousand Eur under  
 346 historical conditions, to 1.7 million Eur in 2050 and almost 26 million Eur in 2100. In our simulations, the  
 347 designed barrier (2.8 m barrier along 7.8 km of coast) was able to avoid most of the damage to residential  
 348 buildings (figure 8, right). The measure becomes less efficient for the most extreme scenarios in 2050 and 2100,  
 349 when the increase in TWL cause the surmounting of the barrier. This assessment does not account for the  
 350 beach resorts and bathing facilities, which are located along the barrier or between the barrier and the sea, and  
 351 thus are equally exposed in both the baseline and the defended scenario; they would likely represent an  
 352 additional 7-25% of the baseline damage.

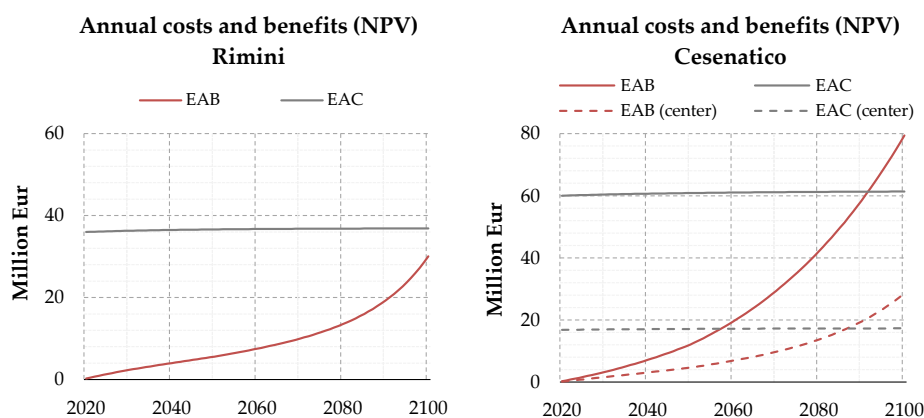


353  
 354 **Figure 9.** Cesenatico: Expected Annual Damage (EAD) according to undefended scenario up to 2100 [left];  
 355 EAD reduction thanks to hazard mitigation offered by the coastal barrier [right].



356 **4.3 Cost-Benefit Analysis**

357 EAD estimates obtained for both the baseline and the defended scenarios enable to run a CBA to evaluate  
 358 mitigation measures in terms of NPV, BCR and payback period for the two time-horizons (30 years and 80  
 359 years). In figure 9, the Expected Annual Benefits (EAB) grow at faster rate approaching 2100 in both sites,  
 360 because of the larger expected damages from more intense, less frequent flood events. The cost of defence  
 361 implementation is repaid by avoided damage after about 70 years in Cesenatico and after 90 years in Rimini.  
 362 In Cesenatico benefits grow proportionally to costs, so that the payback time does not change when  
 363 considering a section of the town or the whole coastal perimeter. At 2100, the BCR is 0.82 for Rimini and 1.66  
 364 for Cesenatico, suggesting an overall profitability of the defence structure implementation over the long term.  
 365 The results in terms of CBR do not differ much when comparing the CBA over a selection of exposed records  
 366 corresponding to the town higher-density area (i.e. Cesenatico historical center). Table 2 summarizes the  
 367 metrics of the assessment for different area extent selections. As specified earlier, this assessment does not  
 368 measure the benefits brought in terms of urban renovation, which are the primary focus of Parco del Mare  
 369 project, but only the direct benefits in terms of flood damage reduction.



370

371 **Figure 10.** Cumulated flood defence costs and expected benefits at Net Present Value for Rimini (left) and  
 372 Cesenatico (right).

373

374 **Table 2.** Summary of CBA for planned or designed seaside defence project in Rimini (all town and south  
 375 section only) and Cesenatico (all town and center only) over a time horizon of 30 and 80 years (2020 to 2050  
 376 and 2020 to 2100).

Metrics	Rimini				Cesenatico			
	All town		South only		All town		Center only	
	2050	2100	2050	2100	2050	2100	2050	2100
Baseline EAD [M EUR]	2.8	32	0.5	14.6	1.7	25.9	0.5	12.4
Defended EAD [M EUR]	2.4	17	0.1	0.9	0.1	0.4	0.1	0.4
Expected Annual Benefits [M EUR]	0.4	15	0.4	13.7	1.6	25.5	0.4	11.9
Sum of EAB (discounted) [M EUR]	5.6	30	4.1	27.8	12.0	79.4	4.7	28.6
Sum of EAC (discounted) [M EUR]	36.6	36.9	36.6	36.9	47.4	47.9	17.1	17.3
Net Present Value [M EUR]	-31.0	-6.8	-32.6	-9.1	-35.3	31.5	-12.4	11.3
Benefit-Cost ratio [-]	0.15	0.82	0.11	0.75	0.25	1.66	0.27	1.66



## 377 5. Conclusion

378 In this study we addressed inundation risk scenarios and measures on two coastal sites located along the  
379 North Adriatic coastal plain of Italy, which is projected to become increasingly exposed to ESL events. Both  
380 locations are expected to suffer increasing economic losses from to coastal inundation triggered by extreme  
381 sea level events unless effective coastal adaptation measures are put in place. To understand the impacts of  
382 upcoming ESL events and the potential benefits of designed coastal projects, we run a CBA comparing the  
383 baseline and the defended scenario in terms of flood losses. The defended scenario accounts for the effect of a  
384 coastal barriers based on the design of the “Parco del Mare”, an urban renovation project under construction  
385 in Rimini. The same type of structure is envisaged and its effects simulated along the coastal perimeter of the  
386 nearby town of Cesenatico. First, we characterised reference ESL events in terms of frequency and intensity  
387 based on local historical observations; then, we projected ESL scenarios to 2050 and 2100, accounting for the  
388 combined effect of eustatic SLR and subsidence rates on the TWL, as obtained from existing local studies. We  
389 produced flood hazard maps estimating maximum flood water extent, water depth and velocity using a high-  
390 resolution hydrodynamic model able to replicate the physics the inundation process. The hazard maps were  
391 fed to the damage model in order to calculate the expected annual damage for both baseline and defended  
392 scenarios. An increase in damage is expected for both urban areas from 2020 to 2100: in Cesenatico the EAD  
393 grows by a factor 96, in Rimini by a factor 49.

394 The results obtained from the CBA on both locations show growing profitability of present project investment  
395 over time, associated with the increase of expected annual damage from intense ESL events: the EAD under  
396 the baseline hypothesis is expected to increase by 3.5-fold in 2050, up to 10-fold in 2100. The benefits brought  
397 by the coastal defence project become much larger in the second half of the century: the EAB grows 6.1-fold in  
398 Rimini, 6.5-fold in Cesenatico, from 2050 to 2100. Avoided losses are expected to match the project  
399 implementation costs after about 70 years in Cesenatico and 90 years in Rimini. Benefits are found to increase  
400 proportionally to costs; the payback period in Cesenatico is the same considering either an investment on the  
401 protection of the whole town or only part of it. Further assessments of these renovation projects should look  
402 to measure the indirect and spill-over effects over the local economy brought by the project, and possibly  
403 account also for the intangible benefits.

## 404 Authors contribution

405 MA, AHE and SB conceptualized the study and designed the experiments. AHE carried out the coastal hazard  
406 modelling. SR advised the model setup and calculation. SB and PM provided required data and expertise  
407 about the case study areas. MA performed the economic risk modelling and wrote the manuscript. SM  
408 supported the CBA calculations. JM and SB managed the funding acquisition and project supervision. All co-  
409 authors have reviewed the manuscript.

## 410 Acknowledgment

411 The research leading to this paper received funding through the projects CLARA (EU’s Horizon 2020 research  
412 and innovation programme under grant agreement 730482), SAFERPLACES (Climate-KIC innovation  
413 partnership) and EUCP – European Climate Prediction system under grant agreement 776613. We want to  
414 thank Luisa Perini for her kind support.



415 **References**

- 416 Amadio M, Scorzini AR, Carisi F, et al (2019) Testing empirical and synthetic flood damage models: the case  
417 of Italy. *Nat Hazards Earth Syst Sci* 19:661–678. <https://doi.org/10.5194/nhess-19-661-2019>
- 418 Antonioli F, Anzidei M, Amorosi A, et al (2017) Sea-level rise and potential drowning of the Italian coastal  
419 plains: Flooding risk scenarios for 2100. *Quat Sci Rev* 158:29–43.  
420 <https://doi.org/10.1016/j.quascirev.2016.12.021>
- 421 Armaroli C, Ciavola P, Perini L, et al (2012) Critical storm thresholds for significant morphological changes  
422 and damage along the Emilia-Romagna coastline, Italy. *Geomorphology* 143–144:34–51.  
423 <https://doi.org/10.1016/j.geomorph.2011.09.006>
- 424 Armaroli C, Duo E (2018) Validation of the coastal storm risk assessment framework along the Emilia-  
425 Romagna coast. *Coast Eng* 134:159–167. <https://doi.org/10.1016/j.coastaleng.2017.08.014>
- 426 Boardman AE, Greenberg DH, Vining AR, Weimer DL (2018) *Cost-Benefit Analysis*. Cambridge University  
427 Press
- 428 Bonaduce A, Pinaridi N, Oddo P, et al (2016) Sea-level variability in the Mediterranean Sea from altimetry  
429 and tide gauges. *Clim Dyn* 47:2851–2866. <https://doi.org/10.1007/s00382-016-3001-2>
- 430 Bos F, Zwaneveld P (2017) *Cost-Benefit Analysis for Flood Risk Management and Water Governance in the*  
431 *Netherlands: An Overview of One Century*. SSRN Electron J. <https://doi.org/10.2139/ssrn.3023983>
- 432 Bouwer LM (2011) Have disaster losses increased due to anthropogenic climate change? *Bull Am Meteorol*  
433 *Soc*. <https://doi.org/10.1175/2010BAMS3092.1>
- 434 Carbognin L, Teatini P, Tomasin A, Tosi L (2010) Global change and relative sea level rise at Venice: What  
435 impact in term of flooding. *Clim Dyn* 35:1055–1063. <https://doi.org/10.1007/s00382-009-0617-5>
- 436 Carbognin L, Teatini P, Tosi L (2009) The impact of relative sea level rise on the Northern Adriatic Sea coast,  
437 Italy. *WIT Trans Ecol Environ* 127:137–148. <https://doi.org/10.2495/RAV090121>
- 438 Carminati E, Martinelli G (2002) Subsidence rates in the Po Plain, northern Italy: the relative impact of  
439 natural and anthropogenic causation. *Eng Geol* 66:241–255. [https://doi.org/10.1016/S0013-7952\(02\)00031-5](https://doi.org/10.1016/S0013-7952(02)00031-5)  
440
- 441 Church JA, White NJ (2011) Sea-Level Rise from the Late 19th to the Early 21st Century. *Surv Geophys*  
442 32:585–602. <https://doi.org/10.1007/s10712-011-9119-1>
- 443 Ciavola P, Coco G (eds) (2017) *Coastal storms: processes and impacts*. Wiley-Blackwell
- 444 CRESME (2014) *Definizione dei costi di (ri)costruzione nell’edilizia*
- 445 Froehlich DC (2002) *IMPACT Project Field Tests 1 and 2: “Blind” Simulation*. 1–18
- 446 Gambolati G, Giunta G, Putti M, et al (1998) Coastal Evolution of the Upper Adriatic Sea due to Sea Level  
447 Rise and Natural and Anthropogenic Land Subsidence. 1–34. <https://doi.org/10.1007/978-94-011-5147-4>
- 448 Garnier E, Ciavola P, Spencer T, et al (2018) Historical analysis of storm events: Case studies in France,  
449 England, Portugal and Italy. *Coast Eng* 134:10–23. <https://doi.org/10.1016/j.coastaleng.2017.06.014>
- 450 Geofabrik GmbH (2018) *OpenStreetMap data extracts*. <http://download.geofabrik.de/>. Accessed 30 Mar 2017
- 451 Hallegatte S, Green C, Nicholls RJ, Corfee-Morlot J (2013) Future flood losses in major coastal cities. *Nat*  
452 *Clim Chang*. <https://doi.org/10.1038/nclimate1979>
- 453 Hinkel J, Lincke D, Vafeidis AT, et al (2014) Coastal flood damage and adaptation costs under 21st century  
454 sea-level rise. *Proc Natl Acad Sci*. <https://doi.org/10.1073/pnas.1222469111>
- 455 Huizinga J, Moel H De, Szewczyk W (2017) *Global flood depth-damage functions : Methodology and the*  
456 *Database with Guidelines*



- 457 IPCC (2019) IPCC Special Report on the Ocean and Cryosphere in a Changing Climate
- 458 Jongman B, Kreibich H, Apel H, et al (2012a) Comparative flood damage model assessment: towards a  
459 European approach. *Nat Hazards Earth Syst Sci* 12:3733–3752
- 460 Jongman B, Ward PJ, Aerts JCJH (2012b) Global exposure to river and coastal flooding: Long term trends  
461 and changes. *Glob Environ Chang*. <https://doi.org/10.1016/j.gloenvcha.2012.07.004>
- 462 Jonkman SN, Brinkhuis-Jak M, Kok M (2004) Cost benefit analysis and flood damage mitigation in the  
463 Netherlands. *Heron* 49:95–111
- 464 Kain CL, Lewarn B, Rigby EH, Mazengarb C (2020) Tsunami Inundation and Maritime Hazard Modelling  
465 for a Maximum Credible Tsunami Scenario in Southeast Tasmania, Australia. *Pure Appl Geophys*  
466 177:1549–1568. <https://doi.org/10.1007/s00024-019-02384-0>
- 467 Kemp AC, Horton BP, Donnelly JP, et al (2011) Climate related sea-level variations over the past two  
468 millennia. *Proc Natl Acad Sci U S A* 108:11017–11022. <https://doi.org/10.1073/pnas.1015619108>
- 469 Kind JM (2014) Economically efficient flood protection standards for the Netherlands. *J Flood Risk Manag*  
470 7:103–117. <https://doi.org/10.1111/jfr3.12026>
- 471 Kirezci E, Young IR, Ranasinghe R, et al (2020) Projections of global-scale extreme sea levels and resulting  
472 episodic coastal flooding over the 21st Century. *Sci Rep* 10:1–12. <https://doi.org/10.1038/s41598-020-67736-6>  
473
- 474 Lambeck K, Antonioli F, Anzidei M, et al (2011) Sea level change along the Italian coast during the Holocene  
475 and projections for the future. *Quat Int* 232:250–257. <https://doi.org/10.1016/j.quaint.2010.04.026>
- 476 Lambeck K, Purcell A (2005) Sea-level change in the Mediterranean Sea since the LGM: Model predictions  
477 for tectonically stable areas. In: *Quaternary Science Reviews*. Pergamon, pp 1969–1988
- 478 Lionello P (2012) The climate of the Venetian and North Adriatic region: Variability, trends and future  
479 change. *Phys Chem Earth* 40–41:1–8. <https://doi.org/10.1016/j.pce.2012.02.002>
- 480 Lowe J (2008) Intergenerational wealth transfers and social discounting: Supplementary Green Book  
481 guidance. HM Treasury, London 3–6
- 482 Lowe J, Gregory J, Flather R (2001) Changes in the occurrence of storm surges around the United Kingdom  
483 under a future climate scenario using a dynamic storm surge model driven by the Hadley Centre  
484 climate models. *Clim Dyn* 18:179–188
- 485 Marsico A, Lisco S, Lo Presti V, et al (2017) Flooding scenario for four Italian coastal plains using three  
486 relative sea level rise models. *J Maps* 13:961–967. <https://doi.org/10.1080/17445647.2017.1415989>
- 487 Masina M, Lamberti A, Archetti R (2015) Coastal flooding: A copula based approach for estimating the joint  
488 probability of water levels and waves. *Coast Eng* 97:37–52.  
489 <https://doi.org/10.1016/j.coastaleng.2014.12.010>
- 490 McGranahan G, Balk D, Anderson B (2007) The rising tide: Assessing the risks of climate change and human  
491 settlements in low elevation coastal zones. *Environ Urban*. <https://doi.org/10.1177/0956247807076960>
- 492 McInnes KL, Walsh KJE, Hubbert GD, Beer T (2003) Impact of sea-level rise and storm surges in a coastal  
493 community. *Nat Hazards* 30:187–207. <https://doi.org/10.1023/A:1026118417752>
- 494 Mechler R (2016) Reviewing estimates of the economic efficiency of disaster risk management: opportunities  
495 and limitations of using risk-based cost–benefit analysis. *Nat Hazards* 81:2121–2147.  
496 <https://doi.org/10.1007/s11069-016-2170-y>
- 497 Meyssignac B, Cazenave A (2012) Sea level: A review of present-day and recent-past changes and variability.  
498 *J. Geodyn*. 58:96–109
- 499 Mitchum GT, Nerem RS, Merrifield MA, Gehrels WR (2010) Modern Sea-Level-Change Estimates. In:



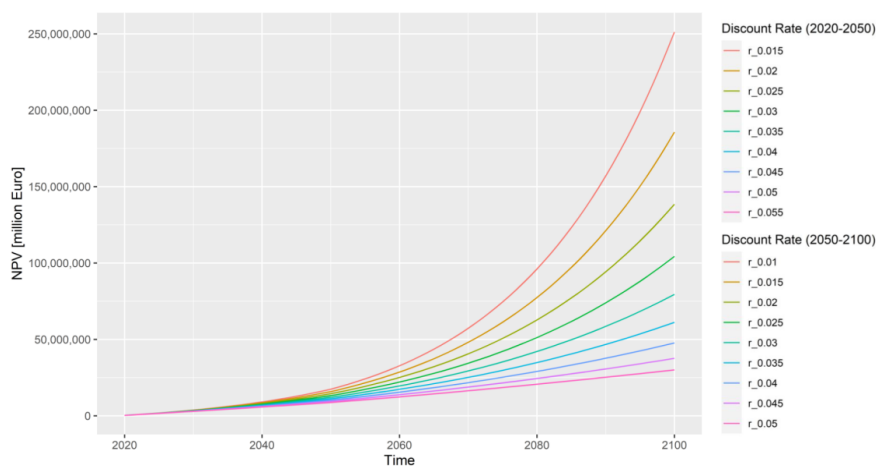
- 500 Understanding Sea-Level Rise and Variability. Wiley-Blackwell, Oxford, UK, pp 122–142
- 501 Muis S, Verlaan M, Winsemius HC, et al (2016) A global reanalysis of storm surges and extreme sea levels.  
502 Nat Commun 7:1–11. <https://doi.org/10.1038/ncomms11969>
- 503 Nicholls RJ, Cazenave A (2010) Sea-level rise and its impact on coastal zones. Science (80- ) 328:1517–1520.  
504 <https://doi.org/10.1126/science.1185782>
- 505 Olsen AS, Zhou Q, Linde JJ, Arnbjerg-Nielsen K (2015) Comparing methods of calculating expected annual  
506 damage in urban pluvial flood risk assessments. Water (Switzerland) 7:255–270.  
507 <https://doi.org/10.3390/w7010255>
- 508 Peltier WR (2004) Global Glacial Isostasy and the surface of the ice-age Earth: the ICE-5G (VM2) Model and  
509 GRACE. Annu Rev Earth Planet Sci 32:111–149. <https://doi.org/10.1146/annurev.earth.32.082503.144359>
- 510 Peltier WR, Argus DF, Drummond R (2015) Space geodesy constrains ice age terminal deglaciation: The  
511 global ICE-6G\_C (VM5a) model. J Geophys Res Solid Earth 120:450–487.  
512 <https://doi.org/10.1002/2014JB011176>
- 513 Perini L, Calabrese L, Deserti M, et al (2011) Le mareggiate e gli impatti sulla costa in Emilia-Romagna 1946-  
514 2010
- 515 Perini L, Calabrese L, Luciani P, et al (2017) Sea-level rise along the Emilia-Romagna coast (Northern Italy) in  
516 2100: Scenarios and impacts. Nat Hazards Earth Syst Sci 17:2271–2287. <https://doi.org/10.5194/nhess-17-2271-2017>
- 517
- 518 Perini L, Calabrese L, Salerno G, Luciani P (2012) Mapping of flood risk in Emilia-Romagna coastal areas.  
519 Rend Online Soc Geol Ital 21:501–502. <https://doi.org/10.13140/2.1.1703.7766>
- 520 Polcari M, Albano M, Montuori A, et al (2018) InSAR monitoring of Italian coastline revealing natural and  
521 anthropogenic ground deformation phenomena and future perspectives. Sustain 10:4–7.  
522 <https://doi.org/10.3390/su10093152>
- 523 Price R (2018) Cost-effectiveness of disaster risk reduction and adaptation to climate change. 1–21
- 524 Roberts S (2020) ANUGA - Open source hydrodynamic / hydraulic modelling. <https://anuga.anu.edu.au/>
- 525 Roberts S, Nielsen O, Gray D, Sexton J (2015) ANUGA User Manual
- 526 Solari L, Del Soldato M, Bianchini S, et al (2018) From ERS 1/2 to Sentinel-1: Subsidence Monitoring in Italy  
527 in the Last Two Decades. Front Earth Sci 6. <https://doi.org/10.3389/feart.2018.00149>
- 528 Stocker TF, Dahe Q, Plattner G-K, et al (2013) Technical Summary. In: Stocker TF, Qin D, Plattner G-K, et al.  
529 (eds) Climate Change 2013: The Physical Science Basis. Contribution of Working Group I to the Fifth  
530 Assessment Report of the Intergovernmental Panel on Climate Change. Cambridge University Press,  
531 Cambridge, United Kingdom and New York, NY, USA., pp 33–115
- 532 Syvitski JPM, Kettner AJ, Overeem I, et al (2009) Sinking deltas due to human activities. Nat Geosci.  
533 <https://doi.org/10.1038/ngeo629>
- 534 Teatini P, Ferronato M, Gambolati G, Gonella M (2006) Groundwater pumping and land subsidence in the  
535 Emilia-Romagna coastland, Italy: Modeling the past occurrence and the future trend. Water Resour Res  
536 42. <https://doi.org/10.1029/2005WR004242>
- 537 Thomson AM, Calvin K V., Smith SJ, et al (2011) RCP4.5: A pathway for stabilization of radiative forcing by  
538 2100. Clim Change 109:77–94. <https://doi.org/10.1007/s10584-011-0151-4>
- 539 Tsimplis MN, Raicich F, Fenoglio-Marc L, et al (2012) Recent developments in understanding sea level rise at  
540 the Adriatic coasts. Phys Chem Earth 40–41:59–71. <https://doi.org/10.1016/j.pce.2009.11.007>
- 541 Tsimplis MN, Rixen M (2002) Sea level in the Mediterranean Sea: The contribution of temperature and  
542 salinity changes. Geophys Res Lett 29:51-1-51–4. <https://doi.org/10.1029/2002gl015870>



- 543 Vousdoukas MI, Mentaschi L, Feyen L, Voukouvalas E (2017) Extreme sea levels on the rise along Europe's  
544 coasts. *Earth's Futur* 5:1–20. <https://doi.org/10.1002/ef2.192>
- 545 Vousdoukas MI, Mentaschi L, Voukouvalas E, et al (2018) Global probabilistic projections of extreme sea  
546 levels show intensification of coastal flood hazard. *Nat Commun* 9:1–12. [https://doi.org/10.1038/s41467-](https://doi.org/10.1038/s41467-018-04692-w)  
547 [018-04692-w](https://doi.org/10.1038/s41467-018-04692-w)
- 548 Wöppelmann G, Marcos M (2012) Coastal sea level rise in southern Europe and the nonclimate contribution  
549 of vertical land motion. *J Geophys Res Ocean* 117:. <https://doi.org/10.1029/2011JC007469>
- 550 Zanchettin D, Traverso P, Tomasino M (2007) Observations on future sea level changes in the Venice lagoon.  
551 *Hydrobiologia*. <https://doi.org/10.1007/s10750-006-0416-5>
- 552

### 553 Appendix A

554 A sensitivity analysis is carried out on the discount rate. Figure A1 below shows how the NPV changes with  
555 discount rate  $r$  ranging from 1.5% to 5.5% (2020 to 2050) and 1% to 5% (2050–2100).



556

557

**Figure A1.** Sensitivity analysis of NPV using a variable discount rate.